柴达木盆地渐新统上干柴沟组碳酸盐纹层成因及古气候意义

何海龙, 郭佩, 李长志, 魏研, 张锡婷, 文华国

相似文章推荐（请使用火狐或IE浏览器查看文章）

Similar articles recommended (Please use Firefox or IE to view the article)

磨圆度定量表征在扇三角洲沉积微相判别中的应用

Application of Quantitative Roundness Characterization to Identify Sedimentary Microfacies in Fan Delta Deposits: A case study of conglomerates in the Baikouquan Formation, Mahu Sag

沉积学报. 2020, 38(5): 956-965   https://doi.org/10.14027/j.issn.1000-0550.2019.111

广丰盆地晚白垩世周田组红层沉积特征及古气候意义

Sedimentary Characteristics and Paleoclimatic Significance of the Late Cretaceous Zhoutian Formation Red Beds in the Guangfeng Basin

沉积学报. 2020, 38(3): 485-496   https://doi.org/10.14027/j.issn.1000-0550.2019.074

小湖盆浅水三角洲沉积特征及其等时格架划分方案——以南堡43区东二段为例

Study on Sedimentary Characteristics of Shallow-water Deltas and Isochronous Stratigraphic Framework: An example of Ed_2 of 4-3 zone of Nanpu oil field

沉积学报. 2019, 37(5): 1079-1086   https://doi.org/10.14027/j.issn.1000-0550.2019.017

柴达木盆地英西地区下干柴沟组上段高频旋回与古地貌特征

High-frequency Cycles and Paleogeomorphic Features of the Upper Member of the Lower Ganchaigou Formation in the Yingxi Area, Qaidam Basin

沉积学报. 2019, 37(4): 812-824   https://doi.org/10.14027/j.issn.1000-0550.2018.174

砾石分析在扇三角洲与湖岸线演化关系中的应用——以准噶尔盆地玛湖凹陷周缘百口泉组为例

The Role of Gravel in Analyzing on the Relationship between Fan Deltas and Lake Shorelines in a Lacustrine Basin: Case study of the Baikouquan Formation around the Mahu Depression in Xinjiang

沉积学报. 2019, 37(3): 550-564   https://doi.org/10.14027/j.issn.1000-0550.2019.005

柴达木盆地渐新统上干柴沟组碳酸盐纹层成因及古气候意义

何海龙[1,2,3],郭佩[1,2,3],李长志[2,4],魏研[3],张锡婷[1,2,3],文华国[1,2,3]

1. 自然资源部深时地理环境重建与应用重点实验室,成都理工大学,成都 610059
2. 油气藏地质及开发工程国家重点实验室,成都理工大学,成都 610059
3. 成都理工大学沉积地质研究院,成都 610059
4. 成都理工大学地球科学学院,成都 610059

摘 要 【目的】纹层是细粒沉积物在湖水分层条件下缓慢沉积的表现,其中碳酸盐纹层对于水体盐度、碱度和生物活动变化敏感,是判断大陆古气候、古水文较为重要的证据之一,但目前针对湖相碳酸盐纹层的研究较少。通过对柴达木盆地湖相碳酸盐纹层进行研究,尤其是碳酸盐纹层中文石、白云石的成因以及碳酸盐纹层的形成机制,由此揭示青藏高原北部渐新世气候—环境变化。【方法】以柴达木盆地西岔沟剖面渐新统上干柴沟组为例,通过常规薄片、荧光薄片和扫描电镜的观察以及X射线粉晶衍射和碳氧同位素分析测试,然后对岩石学特征和碳氧同位素特征进行分析,最终结合西岔沟剖面上干柴沟组碳酸盐矿物含量和碳氧同位素纵向变化情况探讨青藏高原北部渐新世气候—环境变化。【结果】西岔沟剖面上干柴沟组主要发育粉砂、碳酸盐、黏土三种类型纹层,其中碳酸盐纹层中文石、方解石和白云石含量交替富集且均与有机质共生,文石含量较高的样品碳同位素偏正,白云石富集的样品则氧同位素相对较高,且西岔沟剖面上干柴沟组碳酸盐矿物含量和碳氧同位素纵向变化具有一定的规律性。【结论】此次研究为青藏高原北部在渐新世时期气候经历了由早期湿润到晚期(半)干旱的演化过程提供有力的支撑。

关键词 湖相纹层;文石;白云石;藻类勃发;古水文

0 引言

纹层是细粒沉积物在湖水分层条件下缓慢沉积的表现[1-4]。分层的水体最有利于纹层的形成[1,4-6],湖水分层可以造成底部水体严重缺氧,使得底栖动物难以生存,避免了生物扰动破坏纹理[2],从而形成与沉积环境变化有关的沉积纹层[1,6]。纹层的形成过程与水平面变化有关,而湖泊的水位变化和沉积过程又对气候变化(蒸发、降水和河流流入量)极为敏感,因此,可从纹层的矿物成分和厚度中可提取古气候、古环境重要信息。如纹层可用于研究季节到年度尺标的气候变化[1,7],进而为古气候周期、地质事件重现、古湖泊物理、古湖水化学及古生产力的演化研究

提供绝佳材料[5]。近十年来,随着我国页岩油气的勘探开发,纹层对页岩有机质富集、储集性能的影响逐渐被学者关注并重视[8-11]。

单个纹层常见矿物成分包括:来自流域的外来碎屑物质、沉淀的碳酸盐矿物、蒸发岩矿物、富铁富锰的絮凝体、内源的有机碎屑以及从底部重悬的内源和外源碎屑矿物[5]。在湖水分层的条件下,各种藻类、碳酸盐矿物、有机质、黏土矿物等可以在不同的季节形成不同类型的纹层。其中碳酸盐纹层是咸化湖盆沉积中的一种重要纹层类型,包括文石纹层、方解石纹层和白云石纹层,广泛发育于我国渤海湾盆地[2,12-13]、柴达木盆地[14-15],及土耳其Van湖[16]、美国Briger湖[17]和阿尔卑斯Piànico古湖[7]等国外湖泊。碳

酸盐矿物是湖盆古气候变化良好记录的载体[18]，自生碳酸盐矿物的类型和碳氧同位素组成通常被用作重要的古气候指标[19-21]。因此，研究碳酸盐纹层可以更好地恢复湖盆古气候变化。

柴达木盆地是青藏高原北部最大的沉积盆地，自始新世以来盆地内长期发育内流型湖泊，沉积了一套厚达 8 000 m 以上的河湖相沉积。长期以来，前人研究更多地聚焦于盆地内湖相碳酸盐岩（主要是微生物岩和颗粒灰岩）的古气候、古环境和油气储层[22-25]以及始新统下干柴沟组混积岩生烃潜力和页岩储层的研究[26]，对渐新统上干柴沟组碳酸盐岩成因及其古气候的研究相对缺乏。渐新世时期全球气候从始新世的"温室"气候快速转变为"冰室"气候，气候变得异常寒冷[27]。前人认为渐新世气候在逐步变冷且气候持续干旱[17]，然而大多数学者对于青藏高原西北缘的柴达木盆地渐新世（20.0~35.5 Ma）气候的演化过程未能进行细致说明。柴达木盆地西南缘西岔沟（或称花土沟）野外剖面的上干柴沟组出露完整，保存良好，是该剖面沉积最细粒层段，且纹层较为发育[28]。本文以西岔沟剖面上干柴沟组为研究对象，通过常规薄片、荧光薄片和扫描电镜的观察以及 X 射线粉晶衍射和碳氧同位素分析测试，对其中的碳酸盐岩矿物发育程度、矿物学特征和碳氧同位素特征进行研究，探讨碳酸盐岩矿物尤其是文石、白云石的成因以及碳酸盐纹层的形成机制，由此揭示青藏高原北部渐新世气候—环境变化。

1 地质概况

柴达木盆地是青藏高原北部最大的新生代沉积盆地，面积为 12.1×10⁴ km²，平均海拔约 3 km，地处青藏高原东北部的核心部位，主体位于青海省西北部，介于 35°00′~39°20′ N，90°16′~99°20′ E，是一个典型的山间盆地。柴达木盆地北西侧毗邻阿尔金断裂，东北侧和南侧边界分别与祁连山和东昆仑山相接。受青藏高原阶段性隆升和周缘山体不同步挤压的影响，柴达木盆地的沉积中心在新生代不断发生迁移，古近纪期间主湖泊沿着阿尔金断裂不断向东北方向迁移，新近纪期间受阿尔金山隆升的影响主湖泊向东南方向快速迁移[29]。柴达木盆地古近—新近纪湖盆整体以半咸水—咸水沉积环境为主，湖水矿化度较高。由于喜马拉雅山脉自渐新世以来一直隆升[4]，阻止了水汽的运移，盆地环境变得持续干旱[6]，且在渐新

世早期，发育咸化湖泊—盐湖沉积，渐新世中、晚期发育半咸水湖泊与扇三角洲沉积[23]（图 1a）。

西岔沟剖面位于盆地西北端阿尔金山和昆仑山两大山系的交汇部位，阿尔金山南麓，著名的干柴沟断鼻构造西南翼（图 1a，b），是柴达木盆地新生代岩石地层单元组剖面所在地，新生代地层厚度为 4 500 m。实测西岔沟剖面起点坐标 38°26′15.0″ N，90°52′20.5″ E，终点坐标 38°22′49.4″ N，90°53′01.0″ E[28]。柴达木盆地西部西岔沟剖面沉积地层由始新统下干柴沟组至中新统上油砂山组组成，岩性以泥灰岩、灰质泥岩、粉砂岩和粗砂岩为主（图 1c、图 2），偶见含砾砂岩或泥质砂岩，常见泥灰岩与粗砂岩互层。西岔沟剖面记录了一个完整的湖进至湖退的沉积旋回[28]，其中上干柴沟组沉积时期为该剖面最大湖侵期[15]，此次采样以西岔沟剖面上干柴沟组碳酸盐岩为主，由底至顶共计 40 块样品。

2 样品与实验

研究过程中，首先通过普通薄片鉴定，对西岔沟渐新统上干柴沟组岩石进行矿物成分鉴定和成岩作用分析。本次共磨制 40 个常规薄片样品，薄片三分之一部分进行了茜素红染色，用以区分白云石和方解石。在薄片观察的基础上，挑选 16 块样品进行 X 射线粉晶衍射分析，判断各类碳酸盐矿物的含量及关系。通过高精度场发射扫描电镜，对白云石、方解石和文石等矿物形态进行了系统观察，同时结合荧光显微镜对含纹层样品进行有机质观察，以此判断有机质与碳酸盐矿物赋存的关系。最后，对挑选出的 16 块样品进行碳氧同位素检测，以此通过碳氧同位素及其与碳酸盐岩矿物的关系分析古环境及其古气候。

薄片鉴定、扫描电镜观察、荧光分析和 X 射线粉晶衍射（XRD）分析主要在成都理工大学油气藏地质及开发工程国家重点实验室进行。稳定同位素在中科院地质与地球物理研究所稳定同位素地球化学实验室测试。使用质谱型号为 MAT253，所测数据均为相对国际标准 VPDB 之值，内部标准监测显示 $\delta^{13}C$ 和 $\delta^{18}O$ 的标准偏差分别优于 0.15‰ 和 0.20‰。

3 结果

3.1 上干柴沟组纹层矿物组合特征

西岔沟剖面新生代地层的纹层主要发育于上干

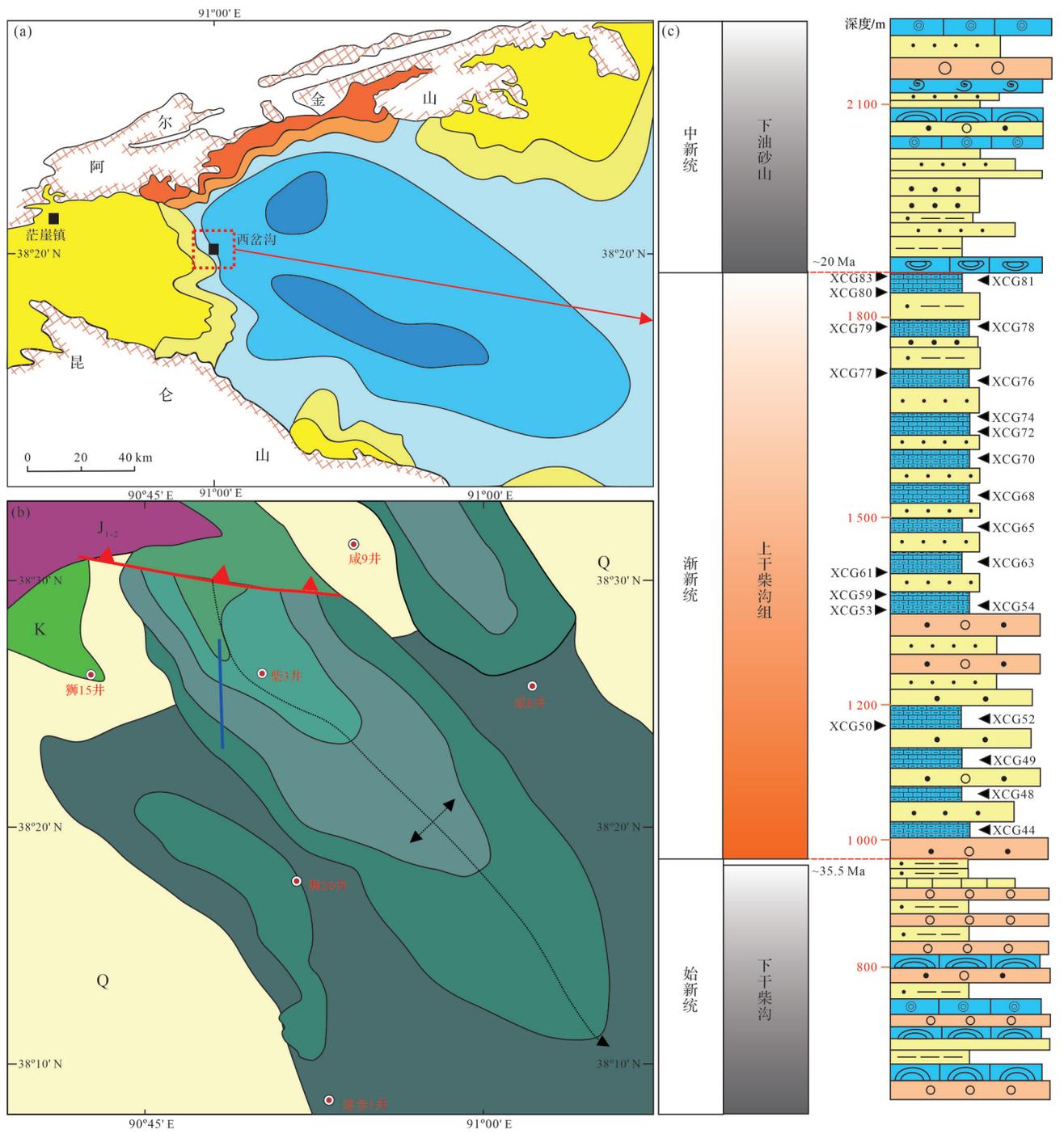图1　研究区位置及岩性地层柱状图

(a)柴达木盆地上干柴沟组沉积相图(据文献[30]修改);(b)西岔沟剖面地层出露情况;(c)西岔沟剖面干柴沟组岩性柱状图

Fig.1　Location of the study areaand lithological column

(a) sedimentary facies diagram of the Ganchaigou Formation on the regional geological mag of the Qaidam Basin (modified from reference [30]); (b) outcrops of the Xichagou section; (c) columnar lithological section of the Gangchaigou Formation in the Xichagou section
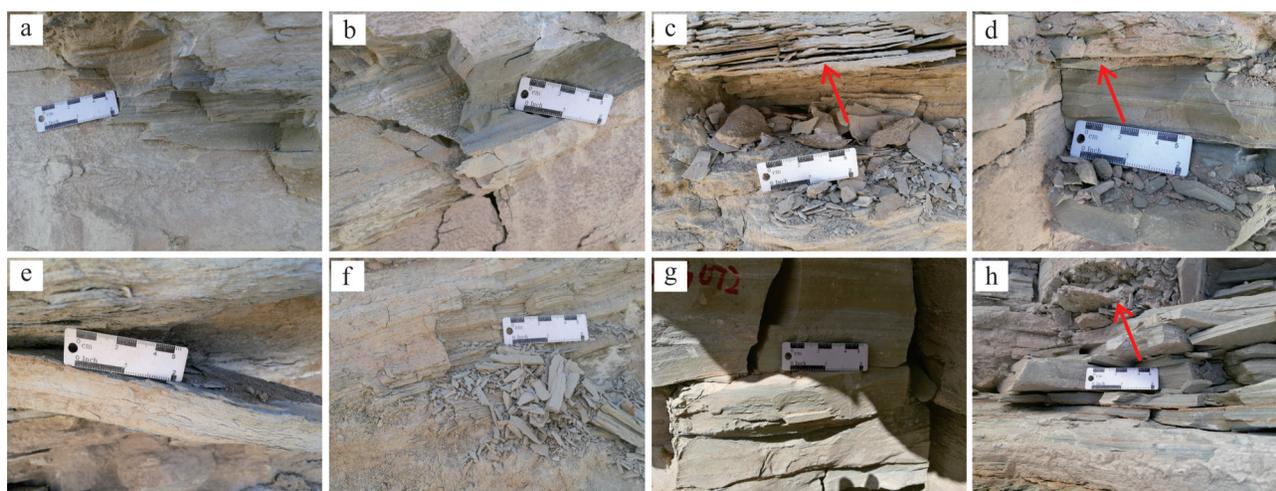
图 2　西岔沟剖面上干柴沟组典型湖相纹层发育照片

(a)XCG051野外样品图片;(b)XCG053野外样品图片;(c)XCG063野外样品图片;(d)XCG065野外样品图片;(e)XCG067野外样品图片;(f)XCG070野外样品图片;(g)XCG072野外样品图片;(h)XCG078野外样品图片;其中红色箭头指向石膏层

Fig.2　Typical laminae pictures of the Shangganchaigou Formation from the Xichagou section

(a)field sample images of XCG051;(b)field sample images of XCG053;(c)field sample images of XCG063;(d)field sample images of XCG065;(e)field sample images of XCG067;(f)field sample images of XCG070;(g)field sample images of XCG072;(h)field sample images of XCG078;with red arrows indicating the gypsum layers

柴沟组的中上部。纹层状岩石以浅黄色、浅绿色为主,是剖面长期风化后的结果(图2)。上干柴沟组常见纹层主要为三类,即粉砂(长英质矿物)纹层、碳酸盐纹层和黏土纹层(图3),大多数纹层以这三端元矿物混积组成,如粉砂纹层中长石和石英碎屑常被方解石或者白云石胶结,白云石纹层中混积有大量长英质颗粒。其中碳酸盐纹层分为方解石纹层(图3b,c)、文石纹层(图3d,j)和白云石纹层(图3e~i),三类纹层均与长英质纹层互层,表现出鲜明的周期性。上干柴沟组纹层通常以平直状或波状产出,厚度变化不均,从 50 μm 到 2 000 μm 不等。

长英质纹层(图3a~i)在单偏光镜下呈浅色,纹层厚度介于 100~2 000 μm,可见大量黏土矿物、石英、长石及少量有机质、白云石、方解石矿物。根据XRD分析结果(表1),石英+长石含量介于 22.6%~57.8%,平均为 36.1%;黏土矿物含量介于 14.4%~37.5%,平均为 23.5%。方解石纹层(图3b,c)单层厚度介于 50~200 μm,厚度变化较大,大多以薄层状产出,该类纹层可含少量白云石矿物和其他碎屑矿物,以及少量有机质和黏土矿物。文石纹层(图3d,f)厚度介于 100~500 μm,该类纹层呈周期性相对较厚层状出现,文石纹层矿物发育单一,陆源碎屑颗粒较少。白云石纹层(图3e,g~i)厚度介于 300~1 000 μm,该类碳酸盐纹层含大量有机质、黏土矿物和少量方解石。根据XRD分析结果(表1),文石含量介

于 3.1%~44%,平均为 9.0%,方解石含量介于 10.1%~41.3%,平均为 18.6%,白云石含量介于 0~41%,平均为 12.3%。整体而言,方解石含量最高,长英质纹层中仍可见方解石矿物(图3b,i)。

3.2　纹层中碳酸盐矿物学特征

高精度扫描电镜观察显示,上干柴沟组较纯的碳酸盐纹层(图4a)以文石组成为主,矿物主要呈长柱状,存在破碎晶体,晶体平均长约 3 μm,长宽比约为 5∶1,晶体表面存在大量似有机质颗粒(图4a,b)。白云石纹层中白云石晶体普遍小于 5 μm(图4c~f),部分小于 1 μm。在显微镜下白云石常常发育于藻团块富集的部位(图3g~i),在高精度扫描电镜下白云石晶体主要分散于黏土矿物基质中(图4d),存在自形白云石晶体被黏土矿物搭桥,白云石晶体的生长挤压薄片状黏土现象(图4e),甚至于白云石晶体内镶嵌黏土矿物(图4f)。在不纯的文石纹层中,长柱状文石晶体被黏土矿物包围(图4g,h),且存在文石与石盐晶体共存现象(图4i)。

3.3　碳酸盐矿物与有机质赋存的关系

西岔沟剖面上干柴沟组有机质较为丰富,类型以菌藻类生物为主,常与碳酸盐矿物共生(图5)。根据有机质赋存类型划分[31],分别有絮团型(图5a~d)、植物碎屑型(图5e)和基质型(图5f)。其中条纹型、絮团型和基质型均属于无定形类,植物碎屑型则属于碎屑类[31]。在方解石纹层与文石纹层中,有机质赋
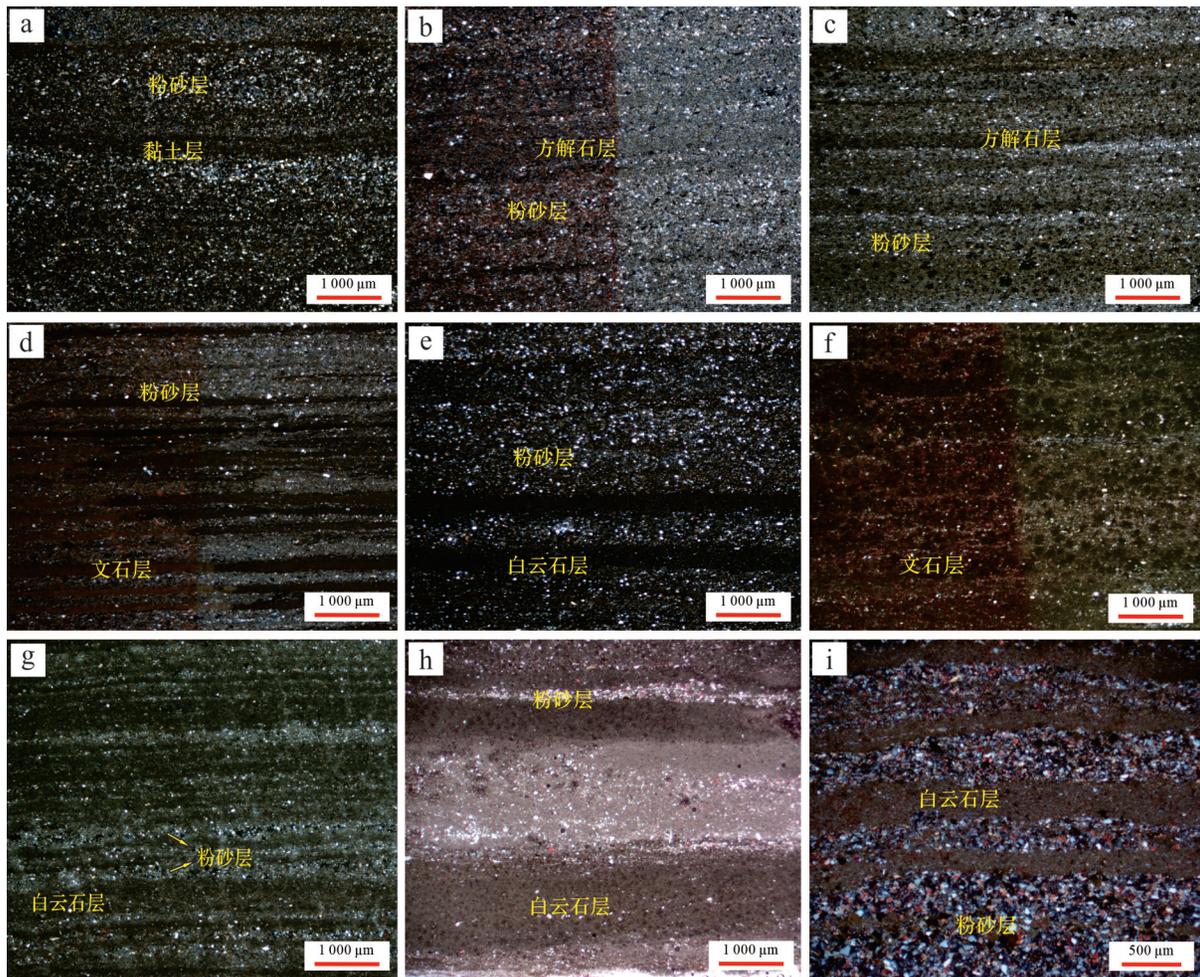
图3　西岔沟剖面上干柴沟组纹层矿物组成特征

(a)泥质粉砂岩,纹层主要由泥质层和粉砂层组成,XCG048样品,单偏光;(b,c)泥质粉砂岩,纹层主要由方解石层和粉砂层组成,b为XCG050样品,正交偏光,c为XCG052样品,正交偏光;(d)泥质粉砂岩,纹层主要由文石层和粉砂层组成,XCG054样品,正交偏光;(e)泥质粉砂岩,纹层主要由白云石层和粉砂层组成,XCG064样品,单偏光;(f)泥质粉砂岩,纹层主要由文石层和粉砂层组成,XCG068样品,正交偏光;(g~i)泥质粉砂岩,纹层主要由白云石层和粉砂层组成,g为XCG072样品,正交偏光,(h)为XCG074样品,单偏光,(i)为XCG078样品,正交偏光

Fig.3　Mineral composition of rock laminae in the Shangganchaigou Formation of the Xichagou section

(a) argillaceous siltstone, the grains are composed of argillaceous and silty layers, sample XCG050, planed-polarized light (PPL); (b, c) Argillaceous siltstone, the lamination is composed of calcite and silty sand layers, (b) is sample XCG050, cross-polarized light (XPL), (c) is sample XCG052, XPL; (d) argillaceous siltstone, composed of aragonite and silty sand layers, sample XCG054, XPL; (e) argillaceous siltstone, the lamination is composed of dolomite and silty sand layers, sample XCG064, PPL; (f) argillaceous siltstone, composed of aragonite and silty sand layers, sample XCG068, XPL; (g-i) The siltstone is composed of dolomite and silty layers; (g) is sample XCG072, XPL; (h) is sample XCG074, PPL; (i) is sample XCG078, XPL

存类型为无定形类,而白云石纹层中有机质赋存类型为碎屑类。有机质内部和边缘常有泥晶方解石(图5d),白云石矿物发育于有机质周围(图5e),文石矿物在有机质中发育(图5f)。

3.4　地球化学特征

西岔沟地区上干柴沟组碳氧同位素总体偏负(表1),全岩 $\delta^{13}C$ 值介于 $-4.07‰\sim2.89‰$,平均值为 $-1.29‰$,全岩 $\delta^{18}O$ 值均偏负,介于 $-7.69‰\sim-2.59‰$,均值为 $-4.88‰$, $\delta^{18}O$ 值和 $\delta^{13}C$ 值相关性较弱。值得注意的是, $\delta^{13}C$ 值偏正的样品均为富文石样品,如样品XCG054、XCG063、XCG068、XCG078(图6)。相较而言,富白云石的样品 $\delta^{18}O$ 值负偏程度较其他样品小。由图6可知,西岔沟地区渐新统上干柴沟组湖相碳酸盐岩碳氧同位素投点落在开放性湖泊和封闭性湖泊之间。相较于前人研究,本次研究上干柴沟组碳酸盐岩氧同位素明显偏正,碳同位素无明显变化,说明此次研究所用样品可信,其氧同位素偏正是因为此次采样位置靠近沉积中心。

表1　西岔沟剖面上干柴沟组XRD与碳氧同位素分析结果

Table 1　X-ray Diffraction (XRD) and carbon and oxygen isotopes of the Shangganchaigou Formation from the Xichagou section

样品编号	分段	成分含量/%								$\delta^{13}C$/‰	$\delta^{18}O$/‰	S盐度/%
		石英	钾长石	斜长石	方解石	白云石	文石	石膏	黏土矿物			
XCG044		22.7	1.1	12.3	41.3	0	0	1.1	21.5	−2.97	−6.79	27.96
XCG053		23.9	1.4	12.6	12.3	22.4	0	1.3	26.1	−2.87	−4.03	30.72
XCG054	第1段	22.3	1.2	11.0	17.9	1.0	21.8	0	24.8	1.74	−6.93	27.82
XCG059		27.7	1.0	11.6	17.2	13.6	4	0	24.9	−1.96	−5.78	28.97
XCG061		33.1	1.5	11.6	14.9	1.4	0	0	37.5	−1.47	−7.69	27.06
XCG063		16.9	2.1	7.3	10.5	4.2	44	0.6	14.4	2.46	−5.35	29.40
XCG065	第2段	34.6	2.0	17.9	13.6	3.3	0	0	28.6	−0.80	−2.59	32.16
XCG068		13.9	0	8.7	19.3	4.1	37	0.5	16.5	2.89	−5.23	29.52
XCG072		18.7	1.1	13.2	14.6	30.2	0	0	22.2	−2.96	−3.75	31.00
XCG074		18.9	0	6.8	11.7	41.0	0	1	20.6	−3.97	−2.69	32.06
XCG076	第3段	23.5	0.6	9.1	20.1	23.3	0	1.3	22.1	−0.76	−5.60	29.15
XCG077		16.7	1.0	9.4	44.0	4.0	0	1.8	23.1	−0.96	−4.87	29.88
XCG078		23.3	2.2	10.7	20.6	4.4	14.8	1.2	22.8	0.38	−6.41	28.34
XCG079		18.1	1.1	7.5	10.1	26.0	19.8	0	17.4	−1.11	−4.09	30.66
XCG080		21.2	1.7	10.9	13.6	28.7	0	0	23.9	−4.07	−3.35	31.40
XCG081	第4段	25.7	1.7	11.3	25.1	9.7	3.1	0	23.4	−2.98	−4.16	30.59
XCG083		39.2	1.8	16.8	11.3	2.7	0	0	28.2	−1.30	−3.16	31.59

4　讨论

4.1　纹层中不同碳酸盐矿物成因探讨

4.1.1　文石和方解石成因

　　湖泊沉积纹层中各类碳酸盐矿物成因解释多样,因湖而异[2-3,7,12-14,16-17,21,40-45](表2),古水文、古气候、古生物意义尚不明确。对国内外各大湖盆调研发现,湖相纹层主要发育于古近纪与第四纪中,澳大利亚McArthur盆地中元古代地层发现了最早的白云石纹层[44]。古近纪发育纹层湖盆分别为中国渤海湾盆地[2,12-13]、中国柴达木盆地[14,40]、中国伦坡拉盆地[42]、美国Sentinel Butte湖[43]和美国Briger盆地[17]。除中国渤海湾盆地和柴达木盆地外,其他湖泊性质均为盐湖,以白云石纹层最为发育,而在古近纪咸水湖中,主要以方解石纹层为主,可见文石纹层,白云石纹层几乎不发育,可见白云石纹层的出现与湖泊高盐度有关。第四纪发育纹层的湖盆主要为中国苏干湖[41]、土耳其Van湖[16]、土耳其Iznik湖[21]、埃塞俄比亚火山口湖[3]、阿尔卑斯山脉Piànico古湖[7]和死海Lisan湖[45],文石纹层主要发育于第四纪湖盆中,这可能与其不稳定性质有关,其中第四纪碱湖以方解石纹层最为发育,且均为碳酸盐沉淀白化事件产生;第四纪盐湖主要为死海Lisan湖[45],以文石纹层发育为主,表明文石的形成也需要极高的盐度;咸水湖主要有中国苏干湖[41]

与埃塞俄比亚火山口湖[3],此两类湖盆中均发育与生物有关的无机成因文石矿物。总之,各类纹层中碳酸盐矿物的成因均与水体强烈蒸发有关[2-3,7,12-14,16-17,21,40-45],且部分湖泊中文石的发育与生物有关[3,14,41]。

　　柴达木盆地上干柴沟组纹层中碳酸盐矿物主要为方解石、白云石和文石。湖泊产生碳酸盐沉淀的必要条件是水体中碳酸盐含量达到饱和至过饱和[46],且不受动力学因素的抑制。湖泊沉积物中碳酸盐矿物的含量受$CaCO_3$含量的季节性变化、湖水盐度及Mg/Ca比值的变化控制[47],随着水中Mg含量的增加,方解石、高Mg方解石和文石依次析出[48]。当湖水中Mg浓度变高时,更趋向于形成文石矿物,文石沉淀速率增加[47-48]。湖泊环境下,高Mg/Ca比主要由蒸发过程中的高盐度引起[14]。前人研究表明,柴达木盆地从路乐河组沉积时期到狮子沟组沉积时期一直处于盐碱化状态,Mg/Ca比值极高[49-50],石盐与文石共存现象(图4i)也说明了文石沉积时处于高盐湖水环境。

　　大部分含文石样品碳同位素比值显示明显正漂移(图6),且样品中文石含量与$\delta^{13}C$值相关系数R值达0.835,指示良好的正相关性(图7)。在相同的水化学条件下,文石一般比同时期形成的低镁方解石和高镁方解石的碳同位素高1‰~2‰[51]。上干柴沟组富集文石样品的$\delta^{13}C$值较其他非富集文石样品碳
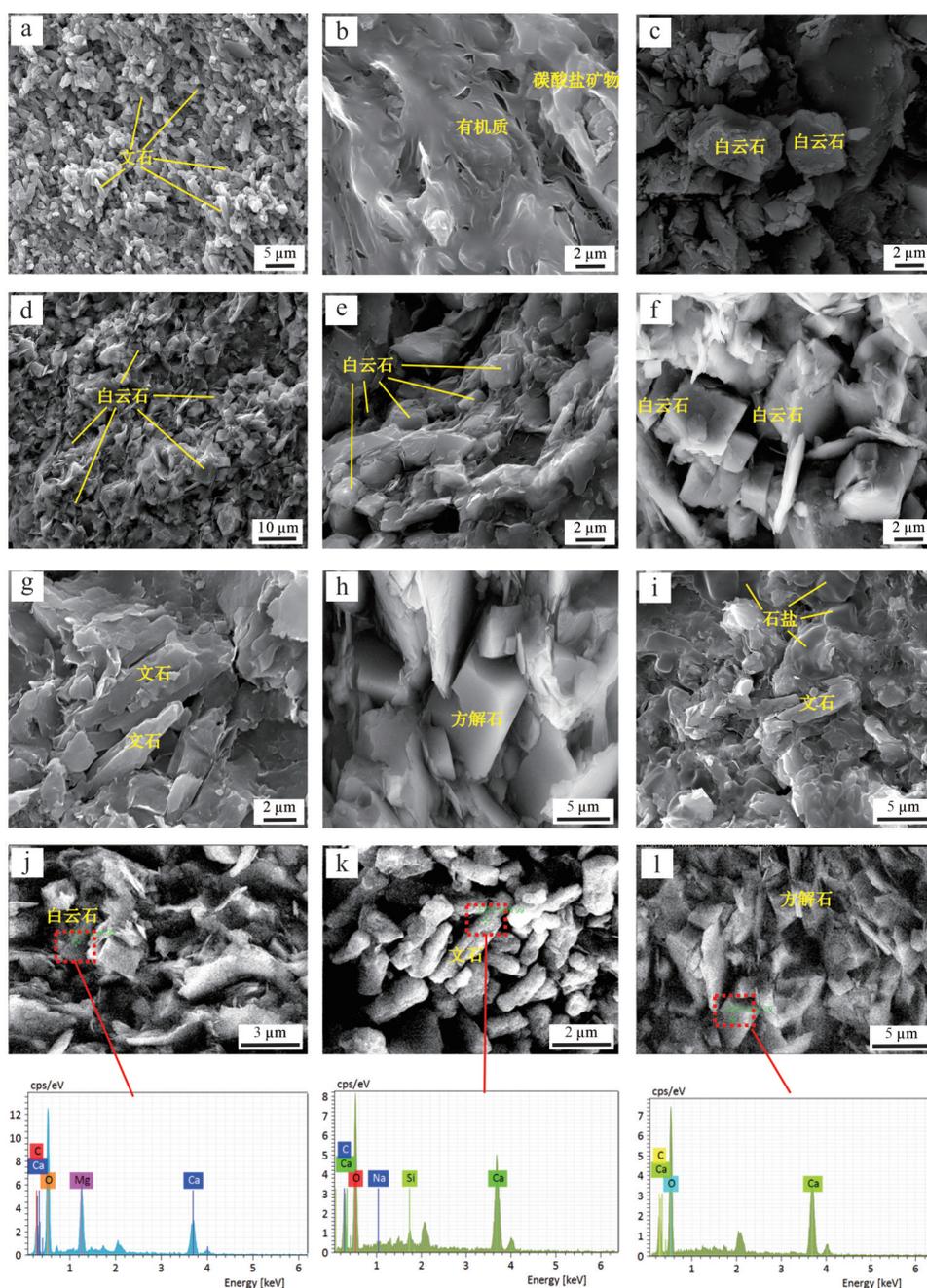
图 4　不同碳酸盐矿物的微观显微特征

(a)碳酸盐纹层以柱状文石为主,XCG078样品,扫描电镜;(b)碳酸盐矿物周围发育大量有机质,XCG078样品,扫描电镜;(c)与碳酸盐纹层互层的碎屑纹层中发育自形白云石晶体,XCG078样品,扫描电镜;(d)云质混积纹层中白云石主要分散于黏土矿物基质中,XCG072样品,扫描电镜;(e)自形白云石晶体被黏土矿物搭桥,白云石晶体的生长挤压薄片状黏土,XCG072样品,扫描电镜;(f)白云石晶体在黏土矿物上生长,XCG072样品,扫描电镜;(g)柱状文石被黏土矿物包围,XCG063样品,扫描电镜;(h)方解石呈块状发育,XCG078样品,扫描电镜;(i)文石与石盐晶体共存,XCG063样品,扫描电镜;(j)白云石矿物特征及其EDS数据,XCG078样品,扫描电镜;(k)文石矿物特征及其EDS数据,XCG078样品,扫描电镜;(l)方解石矿物特征及其EDS数据,XCG078样品,扫描电镜;EDS即为X射线能谱分析

Fig.4　Scanning electron microscope (SEM) images showing different carbonate mineral phases

(a) carbonate grain layer dominated by columnar aragonite in sample XCG078; (b) development of large amounts of organic matter around carbonate minerals in sample XCG078; (c) development of authomorphic dolomite crystals in the detrital grains interlayered with carbonate grains of sample XCG078; (d) dolomite dispersed in clay mineral matrix with the cloudy mélange texture of sample XCG072; (e) authomorphic dolomite crystals bridged by clay minerals, growth of dolomite crystals extruding flaky clay in sample XCG072; (f) dolomite crystals growing on clay minerals in sample XCG072; (g) columnar aragonite in sample XCG063, surrounded by clay minerals; (h) calcite developed in blocks, sample XCG078;(i) coexistence of aragonite and rock salt crystals, sample XCG063;(j) mineral characterization of dolomite and its EDS data, sample XCG078;(k) characterization of the minerals below and their EDS data, sample XCG078;(l) characterization of calcite minerals and their EDS data, sample XCG078; EDS is X-ray energy spectrum analysis
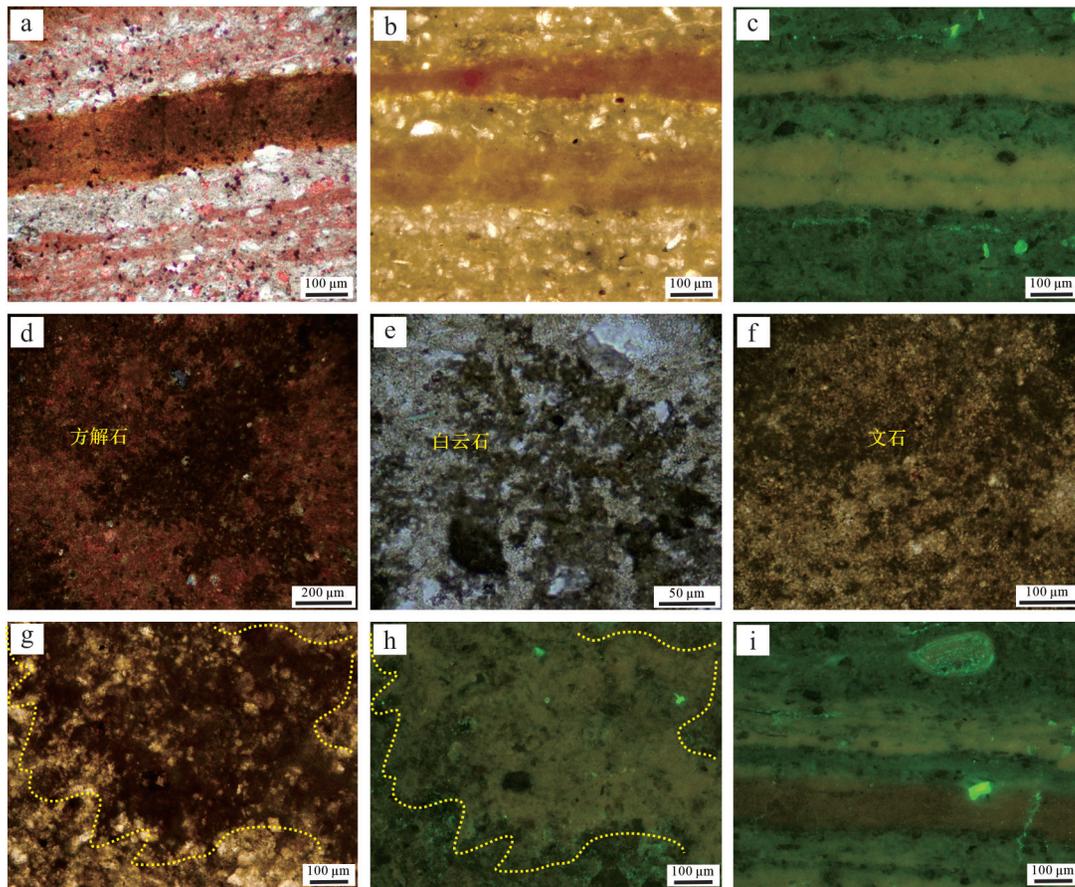
图 5 碳酸盐矿物与有机质的赋存关系

(a)文石纹层中含有大量有机质,XCG078样品,单偏光;(b~c)荧光显微镜下同一视域指示文石纹层发黄色荧光,XCG078样品,b为单偏光,c生屑发强荧光;(d)以方解石占碳酸盐矿物主导的富藻类体样品,XCG078样品,正交偏光;(e)以白云石占碳酸盐物主导的富藻类样品,XCG072样品,单偏光;(f)以文石占碳酸盐矿物主导的富藻类体样品,XCG078样品,单偏光;(g~h)同一视域荧光显微镜下藻类体发黄色荧光,XCG068样品,g为单偏光,h生屑发强荧光;(i)荧光照片指示碳酸盐纹层均发光,但不同碳酸盐纹层发光强弱不同,XCG078样品,生屑发强荧光

Fig.5 Relationship between carbonate minerals and organic matter

(a) sample XCG078 has a large amount of organic matter in the Chinese lithosphere, sample XCG078, single polarized light;(b-c) the same field of view under a fluorescence microscope, indicating that the aragonite layer fluoresces yellow , (b) is sample XCG078, is unipolar; (c) is sample XCG078, the raw debris fluoresces strongly; (d) samples of algal-rich bodies dominated by calcite as a carbonate mineral, sample XCG077, orthogonal polarization; (e) Algae-rich samples dominated by dolomite as carbonate, sample XCG072, single polarized light; (f) samples of algal-rich bodies dominated by aragonite as a carbonate mineral, sample XCG063, single polarized light; (g-h) algal bodies fluoresce yellow under fluorescence microscopy in the same field of view, (g) is sample XCG068,(h) is sample XCG068, strong fluorescence of biopods; (i) fluorescent photographs indicate that the carbonate layers all fluoresce, but the intensity of the fluorescence varies from one carbonate layer to another, sample XCG078, strong fluorescence from raw debris

同位素值高4‰~7‰,说明富文石样品的高$\delta^{13}C$值与文石沉淀造成的碳同位素分馏关系较小,可能与季节性藻类勃发有关。由于浮游藻类勃发会吸收水体中大量的^{12}C,造成湖水暂时性富集^{13}C。文石层在荧光显微镜下发强烈的荧光(图5a~c),在高精度显微镜下可见大量有机质(图4b),鉴于文石矿物含量与碳同位素良好的相关性(7a),认为文石的沉淀与富有生物勃发有关。文石与方解石呈柱状(图4a,b),表明Mg离子含量高[52]。藻类植物的光合作用可诱导方解石和文石的沉淀[46]。在温暖年份,湖水热力分层出现较早且持续时间较长,光合作用细胞对无机碳的吸收会导致

周围环境中CO_2和CO_3^{2-}的浓度梯度较强。细胞周围的微环境也有较高的pH值,这种微环境促进了文石或方解石的沉淀[46],同时还可作为文石或方解石沉淀的结晶核促使碳酸钙快速沉淀[16,46,53]。样品XCG059、XCG079和XCG081的碳同位素值均偏负。其中,样品XCG059和XCG081的文石含量均低于5%,对全岩碳同位素影响较小,故其偏负;而样品XCG079白云石含量最高(26.0%),因白云石对碳同位素组成影响显著,其碳同位素值也偏负。
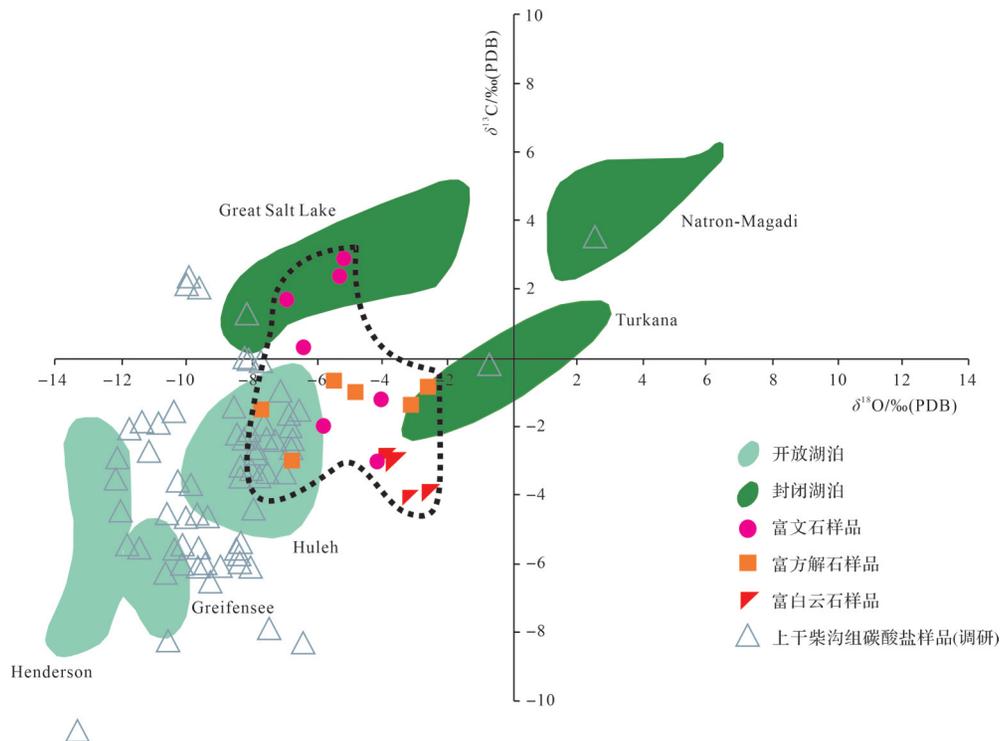
文石在常温常压条件下处于亚稳态,很容易通过新生变形作用或溶解作用转变为方解石[21,54],因此

图 6 柴达木盆地西岔沟剖面上干柴沟组湖相碳酸盐岩碳氧同位素组成与沉积环境分析
(据文献[32-33]修改,其他碳酸盐样品数据来源于文献[34-39])

Fig.6 Carbon and oxygen isotopes and depositional environments for the Shangganchaigou Formation of the Xichagou section in the Qaidam Basin (modified from references [32-33], other carbonate sample data from references [34-39])

在第四纪以前的地层中很少出现,但在我国柴达木盆地和美国绿河盆地始新统中均有保存[14,17],主要为湖泊原始沉降产物。文石在较老地层中的溶解、保存和富集受多种因素的影响,如孔隙水酸碱度变化、有机质微生物降解、沉积速率、岩性以及地温梯度等[55-58]。一般认为,还原环境、有机质的存在或者孔隙水中较高的 Mg/Ca 比值均有利于文石的保存[7,14,45]。通过扫描电镜观察到文石矿物与石盐类矿物共生(图 4i),推测文石周围孔隙水的盐度较高,且通过常规薄片观察,原文石纹层的上下纹层均为含大量黏土矿物的长英质纹层(图 3d,f),扫描电镜下黏土矿物呈片状(图 4g,h),片状黏土矿物组成致密层,可以有效阻止文石周围的孔隙水物质交换[59]。同时,文石保存的纹层或局部区域有机质异常丰富(图 5a~c),有机的微生物降解迅速消耗氧气,形成缺氧环境,同样有利于文石的保存。

4.1.2 白云石成因

柴达木盆地新生代不同地层均含有一定量的白云石,其中下干柴沟组的白云石研究程度最高,普遍被认为是准同生期交代成因[22,32]或生物诱导原生成

因[22],主要为半开放—半封闭的咸化环境下于水/沉积物界面附近由方解石交代而成的低温白云石。西岔沟剖面上干柴沟组白云石晶体以自形为主,大小约 3 μm,与方解石密切共生,上述矿物学特征与柴达木盆地下干柴沟组的白云石较为相似,指示二者成因可能相同。在西岔沟剖面,上干柴沟组富白云石样品 $\delta^{18}O$ 值的偏负程度较贫白云石样品的样品 $\delta^{18}O$ 值小(表 1、图 6),$\delta^{13}C$ 值较贫白云石样品偏负。氧同位素的变化在湖相沉积体系中反映了湖泊的水文平衡状态,即蒸发量与注入量的变化,一般蒸发作用使湖水 $\delta^{18}O$ 值增加,湖泊外来补水会造成其氧同位素组成变轻[32,60]。上干柴沟组富白云石与富 ^{18}O 的机制相同,说明白云石的形成与蒸发作用有关。前人研究表明湖相碳酸盐岩白云化流体主要有 4 类,即原始湖泊流体、外来淡水、热水热液和海源流体[61]。柴达木盆地渐新世流体应为原始湖泊流体或外来淡水两类,柴达木盆地古近系沉积环境为湖相沉积,且未见有关火山活动报导,故排除热水热液和海源流体。原始湖泊流体是指原始存在的淡水湖泊经过不断蒸发浓缩,进而咸化形成的白云石化流体;外来淡水即来源于湖泊之外的未被咸化的水体[61]。柴达木盆地

表2　湖相沉积中各类碳酸盐纹层特征

Table 2　Research status of various carbonate laminae in lacustrine sediments

| 地区	碳酸盐纹层类型	时代	湖泊类型	纹层基本特征	成因	文献来源
中国渤海湾盆地	方解石纹层	古近纪	咸水湖	东营凹陷:方解石纹层与黏土纹层、有机质纹层、粉砂纹层互层;纹层厚度为10~800 μm;方解石纹层为非纯方解石矿物。束鹿凹陷:方解石层与碎屑层互层,方解石层为纯方解石矿物,纹层组合厚度100~300 μm	东营凹陷:与生物有关的无机成因。束鹿凹陷:受水文气候变化影响的正常湖相沉积	王慧中等[2];孔祥鑫等[12];王伟庆[13]
中国柴达木盆地	文石纹层	古近纪	咸水湖	纹层厚度约为0.1 mm;晶体呈针状,存在破碎晶体,长约3~12 μm;文石纹层为非纯文石矿物;与碎屑层互层	与生物有关的无机成因	Ma et al.[14]
	方解石纹层	古近纪	咸水湖	陆源碎屑纹层和纯碳酸盐纹层互层,纯碳酸盐为它形方解石晶粒构成,粒度一般为0.03~0.06 mm	与生物有关的无机成因	刘占国等[40]
中国苏干湖	白云石纹层	第四纪	咸水湖	平均厚度为1.83 mm,白云石层为纯白云石,与碎屑层互层	水体经强烈蒸发正常湖相沉积	Zhou et al.[41]
	文石纹层	第四纪	咸水湖	平均厚度1.96 mm,为纯文石矿物,与有机质层互层	与生物有关的无机成因	
	方解石纹层	第四系	咸水湖	平均厚度2.5 mm,为纯方解石矿物,与碎屑层互层	水体经强烈蒸发正常的湖相沉积	
中国伦坡拉盆地	白云石纹层	古近纪	盐湖	白云石晶体约2~5 μm,白云石层为非纯白云石矿物;纹层厚0.10~0.15 mm;与富有机物层和硅质碎屑层交替	在浅水环境下水体经强烈蒸发沉积,白云石在有机基质和/或黏土基质表面成核	Wen et al.[42]
土耳其Van 湖	方解石纹层	第四纪	碱湖	方解石晶体约1~10 μm;方解石层为纯方解石矿物;与碎屑层互层	碳酸盐沉淀白化事件(whitings)	Stockhecke et al.[16]
土耳其Iznik湖	文石纹层	第四纪	碱湖	文石晶体呈针状,长约2~10 μm;文石层为非纯文石矿物;与碎屑层互层	受水文气候变化影响的正常湖相沉积	Roeser et al.[21]
美国Sentinel Butte湖	白云石纹层	古近纪	盐湖	纹层厚约0.1~2.0 mm;与有机质层互层	白云石化方解石	Bruce[43]
美国Briger 盆地	文石纹层	古近纪	盐湖	文石晶体为5~10 μm的棱柱形针状;平均层厚0.05~0.30 mm;文石层为非纯文石矿物;与碎屑层互层	水体经强烈蒸发正常的湖相沉积	Murphy et al.[17]
	白云石纹层	古近纪	盐湖	纹层厚度约为0.3 mm;白云石晶体小于15 μm,原生白云石由未固结、分选良好的自形到半自形晶体组成;与碎屑层互层	水体经强烈蒸发正常的湖相沉积	
	方解石纹层	古近纪	盐湖	方解石层与碎屑层互层;平均层厚0.4~0.8 mm;方解石晶体约2~10 μm;方解石层为非纯方解石矿物	水体经强烈蒸发正常的湖相沉积	
埃塞俄比亚火山口湖	文石纹层	第四纪	咸水湖	纹层厚度小于1 mm;文石纹层为非纯文石矿物;与海藻碎屑层互层	与生物有关的无机成因	Lamb et al.[3]
澳大利亚McArthur Basin	白云石纹层	中元古代	咸水湖	白云石颗粒约为0.01~0.20 mm;纹层厚约7 mm;与富有机质泥岩层互层	水体经强烈蒸发正常湖相沉积	Jackson[44]
阿尔卑斯山脉Piànico古湖	方解石纹层	第四纪	碱湖	方解石层与碎屑层互层;平均层厚0.56 mm;方解石层为纯方解石矿物	碳酸盐沉淀白化事件(whitings)	Brauer et al.[7]
死海Lisan湖	文石纹层	第四纪	盐湖	文石晶体呈针状;文石层为纯文石矿物;与碎屑层互层	水体经强烈蒸发正常湖相沉积	Prasad et al.[45]
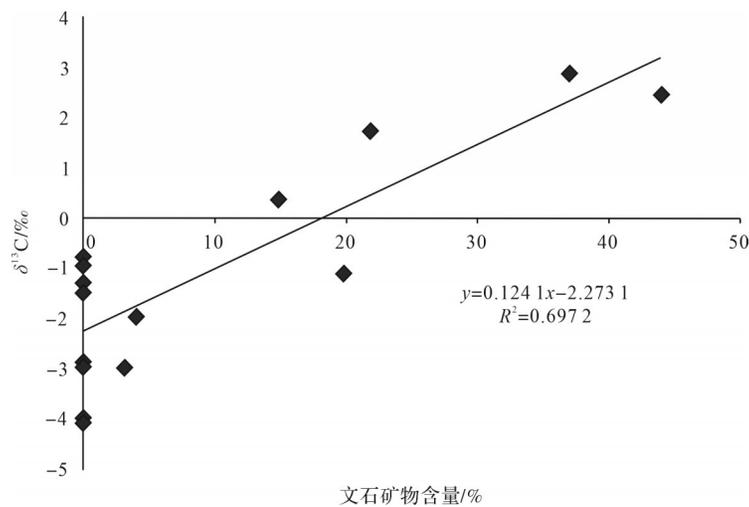
图7　文石含量与碳同位素关系

Fig.7　Relationship between aragonite content and carbon isotopes

夏季受外流水体补给而变为半封闭性湖泊,夏季蒸发作用使得表层水体盐度上升形成重盐水,CaCO₃达到饱和,随着方解石的不断沉淀消耗大量Ca²⁺,Mg/Ca比上升,Mg²⁺析出,促进CaCO₃被交代[61-62]。本研究中富白云石样品碳同位素偏负、氧同位素偏正,也表明此类白云石为准同生交代成因。因此,研究区白云石主要为原始湖泊或周期性外来淡水带来镁离子使得湖泊内形成富镁流体交代方解石形成。

4.2　西岔沟上干柴沟组不同纹层形成机制

古近纪期间柴达木盆地内的主湖泊在东昆仑山向北挤压和阿尔金山断裂韧性左行走滑的共同作用下向西北方向迁移,至上干柴沟组沉积时期已到达西岔沟剖面所在的地区[29]。该时期的湖泊为一个碎屑物质供应充足的咸化湖泊,一方面受阿尔金山东西向山体隆升的影响,不断接受碎屑物质的供应,另一方面湖水盐度已达到碳酸盐矿物饱和浓度,可形成大量自生碳酸盐矿物,因此上干柴沟组的纹层以混积为主。上干柴沟组长英质矿物和黏土矿物含量协同变化,表明其均为季节性径流携带碎屑物质进入湖泊分层水体时形成。较粗的颗粒(沙砾、粗粉砂)在河口附近沉积,形成三角洲沉积体,而细粉砂和黏土矿物则可保持较长时间的悬浮,分布在整个湖泊。

由上述讨论可知,方解石矿物形成时期的水体盐度相对较淡,可能是由于淡水河流流入,覆盖在密度较大的咸水湖水体上,流入水体携带碎屑矿物并提供溶解的Ca²⁺离子,随后导致碳酸盐沉淀[16]。春夏季节伴随着硅藻繁盛和强烈蒸发作用引起碳酸盐过

饱和度增加导致方解石或文石在水体表层大量沉淀。在特别干旱年份,强烈的蒸发作用使得表层水体盐度上升形成重盐水并交代早先形成的方解石或文石,最终形成白云石矿物。随后在秋冬季节因冰面冻结,湖水出现盐度分层,水体几乎处于静态;同时,冬季外流水体的减少和水体的去营养化使得水体密度降低,从而碳酸盐矿物开始随着有机质碎屑等缓慢沉降,形成碳酸盐矿物与黏土矿物等组成的碳酸盐纹层。

碳酸盐纹层到长英质纹层的逐渐转变可能表明,在外来补给水体增加条件下,有更多的碎屑被带入湖中;同时,不同纹层中的不同矿物成分(表1)和稳定同位素漂移(图6)记录了湖泊水体中可能的季节性环境变化。碳酸盐纹层(图3a~i)中碳酸盐矿物、黏土矿物及有机质代表了寒冷季节较少外来水体补给状态。长英质纹层(图3a~i)中保存的长英质矿物、黏土矿物和零星的有机质表明温暖季节较多外来水体补给状态。

4.3　纹层的环境气候指示意义

4.3.1　古水文意义

碳氧同位素的相关性反映了封闭水体长停留时间对同位素演化的影响[63],故可以根据湖相碳酸盐岩的碳氧同位素研究湖泊水文开放与封闭和大气降水/蒸发比(P/E)[20]。由图6可知,西岔沟地区渐新统上干柴沟组湖相碳酸盐岩碳氧同位素投点落在开放性湖泊和封闭性湖泊之间,其相关性差,表明西岔沟地区渐新世沉积时期湖盆水体为半封闭性半开放环境,根据纹层判断湖泊水体开放性具有季节性变化。

湖相碳酸盐岩的碳氧同位素已成为研究古沉积环境变化的重要指标,广泛应用于古湖泊的温度、盐度和气候的恢复[64]。Keith et al.[60]提出利用碳酸盐岩的$\delta^{18}O$和$\delta^{13}C$区分咸水碳酸盐岩和淡水碳酸盐岩的公式$Z=2.048\times(\delta^{13}C+50)+0.498\times(\delta^{18}O+50)$。$Z$值大于120时,为咸水碳酸盐岩;$Z$值小于120时,为淡水碳酸盐岩。据前人研究数据[6,18,32,34-39]和本研究所用数据计算出研究区下干柴沟组Z值均值为118.622[6,18,32,34-39],上干柴沟组Z值均值为117.547[6,18,37-39],下油砂山组Z值均值为119.105[6,37-39],上油砂山组Z值均值为122.681[6,36-39],狮子沟组Z值均值为126.132[34-36]。利用盐度公式$S=\delta^{18}O_{PDB}+21.2/0.61$[62]可以计算出研究区下干柴沟组平均盐度为28.64‰[6,18,32,37-39],上干柴沟组平均盐度为26.99‰[6,18,37-39],下油砂山组平均盐度为27.82‰[6,37-39],上油砂山组平均盐度为29.47‰[6,36-39],狮子沟组平均盐度为32.19‰[34-36]。由此判断上干柴沟组整体处于微咸水环境,在之后的沉积中,盐度不断升高,到狮子沟组沉积时盐度高达32.19‰。值得注意的是,本研究所得Z值整体较前人大,上干柴沟组Z值为122.389,而纪有亮等[38]分析西岔沟剖面Z值为120.850,赵加凡等[37]分析西岔沟剖面Z值均值为126.142,Risesr et al.[6]分析红三旱剖面和干柴沟剖面Z值均值为118.142,毛玲玲等[18]分析大红沟剖面Z值为114.860,肖路安[39]分析红沟剖面Z值均值为115.467。此次所采集样品更加靠近原始湖泊中心[50],氧同位素偏正,因此本研究所得Z值较前人计算Z值大。如表1所示,根据石英和长石碎屑矿物和文石、方解石和白云石含量以及全岩碳氧同位素比值的纵向变化,可将柴达木盆地西岔沟剖面上干柴沟组的沉积演化分为四个阶段,每个阶段对应不同的水体盐度,第一阶段平均盐度约为28.5‰,第二阶段约为30.4‰,第三阶段约为30.2‰,第四阶段约为31.2‰,即渐新统水体盐度总体也处于上升阶段。

4.3.2　古气候指示意义

受水体蒸发和生物勃发的影响,文石的形成和保存包含了大量的古气候和古环境信息[17,65],Zhou et al.[41]通过对柴达木盆地苏干湖碳酸盐纹层的研究认为,文石纹层主要发育于湖水高盐度阶段,且气候为炎热的夏季;而方解石纹层主要发育于淡水环境,发育于春夏初秋季节。Murphy et al.[17]通过对美国怀俄明州Briger盆地始新世绿河组Wilkins Peak段向

Laney段过渡岩层中碳酸盐纹层类型研究发现,方解石主要沉积于湖水蒸发早期,随着Mg/Ca比值的增加,文石和白云石开始形成,说明碳酸盐矿物的转变与气候的变化密切相关。

根据石英和长石碎屑矿物,文石、方解石和白云石含量以及全岩碳氧同位素比值的纵向变化,可将柴达木盆地西岔沟剖面上干柴沟组的沉积演化分为四个阶段(图8):第一阶段(样品XCG044~XCG061),以长英质矿物含量超过40%和全岩氧同位素较低为特征,说明此阶段碎屑矿物输入量较高,水体盐度较低(表1),推断该时期以相对湿润气候为主。第二阶段(样品XCG062~XCG070),以低碎屑矿物、低白云石、高文石和高碳同位素为特征,文石含量的变化受控于气候的变化[67],前文(4.1.1节)已论及纹层中文石矿物在黏土矿物与有机质的影响下得以保存下来,因此文石含量变高,暗示了一个温暖湿润、湖泊水位较高的水文气候环境[63],推断该时期对应最高的湖泊水位且仍以相对湿润气候为主。第三阶段(样品XCG071~XCG079),以低长英质矿物、高白云石含量和高氧同位素比值为特征,对应湖泊低水位和相对高盐度时期,推断该时期以相对干旱气候为主。第四阶段(样品XCG080~XCG083),与第一阶段相似,以长英质矿物含量超过40%为特征,说明陆源碎屑含量输入再次增加。由于西岔沟剖面下油砂山组以浅水碳酸盐岩和三角洲砂岩为主,表明其在上干柴沟组末期发生湖退现象,第四阶段陆源碎屑的增加指示气候不再潮湿。

宋华颖等[28]研究表明,湖水面自下干柴沟组沉积期开始上升,至上干柴沟组早中期上升到最高点,之后相对湖水面逐渐下降,湖水面的变化说明柴达木盆地在渐新统上干柴沟组早期气候湿润,中期开始干旱。这与Song et al.[54]对柴达木盆地渐新世早期气候湿润的研究结果相吻合,Wu et al.[68]根据δ^2H的研究也证实渐新世气候整体变化为湿润到干旱再到湿润。据前人研究数据[6,18,37-39]和本研究所用数据计算Z值和S值也可说明上干柴沟组沉积早期气候较为湿润,中后期气候变得持续干旱。西岔沟剖面上干柴沟组记录了柴达木盆地在渐新世期间气候由早期湿润转变为半干旱,与全球渐新世气候变化相吻合,说明渐新世期间青藏高原北缘并未隆升至现今高度。
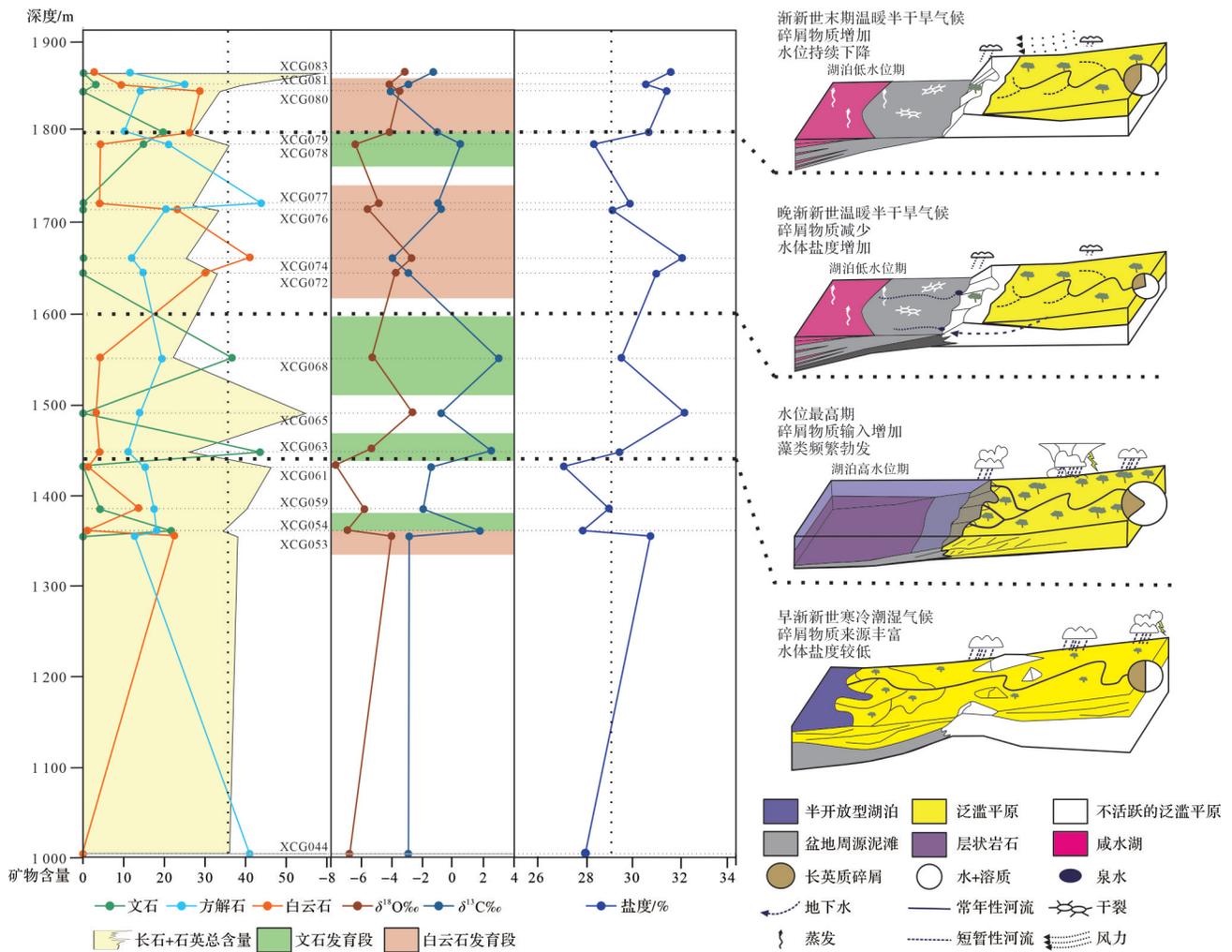
图8 西盆沟剖面上干柴沟组湖泊演变(据文献[66]修改)和气候变化

Fig.8 Lake evolution (modifies from reference [66]) and climate changes of the Shanghanchaigou Formation in the Xichagou section

5 结论

(1)柴达木盆地上干柴沟组发育多种类型的湖相纹层,以碳酸盐纹层和长英质纹层互层为主,大部分纹层矿物成分不纯,以陆源碎屑和自生碳酸盐矿物混积为主。

(2)上干柴沟组纹层中文石、方解石和白云石,其形成和保存与水体化学组成(如Mg/Ca比值)和藻类生物活动有关。在整体咸水环境下,当外界补给水量多于蒸发量时,水体Mg/Ca降低,盐度下降,营养输入增加,方解石和文石矿物开始沉淀并发生转化,其中文石矿物在渐新世地层中得以保存主要与藻类勃发和大量有机质存在有关。当蒸发量大于补给量时,水体中Mg/Ca比值升高,盐度上升,白云石通过交代方解石、文石或自生而形成。

(3)渐新世期间,柴达木盆地气候与全球气候变化一致,早期以湿润气候为主,晚期以半干旱气候为主。西盆沟地区湖泊经历了由低水位至高水位再至低水位的演化过程,早期低水位阶段代表陆源输入较多的浅湖微咸水沉积,中期高水位阶段代表方解石和文石较发育的微咸水沉积,晚期低水位阶段代表陆源输入较少的浅湖咸水沉积。

参考文献(References)

[1] 王冠民,钟建华. 湖泊纹层的沉积机理研究评述与展望[J]. 岩石矿物学杂志,2004,23(1):43-48.[Wang Guanmin, Zhong Jianhua. A review and the prospects of the researches on sedimentary mechanism of lacustrine laminae[J]. Acta Petrologica et Minera-

logica, 2004, 23(1): 43-48.]

[2] 王慧中,刘青春. 牛38井沙三中亚段上部红,灰韵律层的初步研究[J]. 复式油气田,1993,4(2):1-13.［Wang Huizhong, Liu Qingchun. Preliminary research on the brown-grey lacustrine rhythmic deposit of the well Niu-38 in the Upper part of Es$_3^M$, in Shengli petroleum province[J]. Oil Gas Field, 1993, 4(2): 1-13.］

[3] Lamb H, Kebede S, Leng M, et al. Origin and isotopic composition of aragonite laminae in an Ethiopian crater lake[M]//Odada E O, Olago D O. The east African great lakes: Limnology, palaeolimnology and biodiversity. Dordrecht: Springer, 2002: 487-508.

[4] Sun X J, Wang P X. How old is the Asian monsoon system?—Palaeobotanical records from China[J]. Palaeogeography, Palaeoclimatology, Palaeoecology, 2005, 222(3/4): 181-222.

[5] Anderson R Y, Dean W E. Lacustrine varve formation through time[J]. Palaeogeography, Palaeoclimatology, Palaeoecology, 1988, 62(1/2/3/4): 215-235.

[6] Rieser A B, Bojar A V, Neubauer F, et al. Monitoring Cenozoic climate evolution of northeastern Tibet: Stable isotope constraints from the western Qaidam Basin, China[J]. International Journal of Earth Sciences, 2009, 98(5): 1063-1075.

[7] Brauer A, Mangili C, Moscariello A, et al. Palaeoclimatic implications from micro-facies data of a 5900 varve time series from the Piànico interglacial sediment record, southern Alps[J]. Palaeogeography, Palaeoclimatology, Palaeoecology, 2008, 259 (2/3): 121-135.

[8] 何文渊,冯子辉,张金友,等. 松辽盆地北部古龙凹陷古页8HC井地质剖面特征[J]. 油气藏评价与开发,2022,12(1):1-9.［He Wenyuan, Feng Zihui, Zhang Jinyou, et al. Characteristics of geological section of well-GY8HC in Gulong Sag, northern Songliao Basin[J]. Reservoir Evaluation and Development, 2022, 12(1): 1-9.］

[9] 柳波,吕延防,孟元林,等. 湖相纹层状细粒岩特征、成因模式及其页岩油意义:以三塘湖盆地马朗凹陷二叠系芦草沟组为例[J]. 石油勘探与开发,2015,42(5):598-607.［Liu Bo, Lü Yanfang, Meng Yuanlin, et al. Petrologic characteristics and genetic model of lacustrine lamellar fine-grained rock and its significance for shale oil exploration: A case study of Permian Lucaogou Formation in Malang Sag, Santanghu Basin, NW China [J]. Petroleum Exploration and Development, 2015, 42(5): 598-607.］

[10] 李婷婷,朱如凯,白斌,等. 酒泉盆地青西凹陷下沟组湖相细粒沉积岩纹层特征及研究意义[J]. 中国石油勘探,2015,20(1):38-47.［Li Tingting, Zhu Rukai, Bai Bin, et al. Characteristics and research significance of fine lacustrine sedimentary rock laminations of Xiagou Formation in Qingxi Depression of Jiuquan Basin[J]. China Petroleum Exploration, 2015, 20(1): 38-47.］

[11] 赵贤正,蒲秀刚,周立宏,等. 深盆湖相区页岩油富集理论、勘探技术及前景:以渤海湾盆地黄骅坳陷古近系为例[J]. 石油学报,2021,42(2):143-162.［Zhao Xianzheng, Pu Xiugang, Zhou Lihong, et al. Enrichment theory, exploration technology and prospects of shale oil in lacustrine facies zone of deep basin: A case study of the Paleogene in Huanghua Depression, Bohai Bay Basin[J]. Acta Petrolei Sinica, 2021, 42(2): 143-162.］

[12] 孔祥鑫,姜在兴,韩超,等. 束鹿凹陷沙三段下亚段细粒碳酸盐纹层特征与储集意义[J]. 油气地质与采收率,2016,23（4）:19-26.［Kong Xiangxin, Jiang Zaixing, Han Chao, et al. Laminations characteristics and reservoir significance of fine-grained carbonate in the lower 3rd member of Shahejie Formation of Shulu Sag[J]. Petroleum Geology and Recovery Efficiency, 2016, 23(4): 19-26.］

[13] 王伟庆,刘惠民,刘雅利,等. 东营凹陷古近系页岩碳酸盐纹层内部结构与成因[J]. 油气地质与采收率,2022,29（3）:11-19.［Wang Weiqing, Liu Huimin, Liu Yali, et al. Texture and genesis of Paleogene lacustrine shale carbonate laminae in Dongying Sag, Jiyang Depresion, Bohai Bay Basin[J]. Petroleum Geology and Recovery Efficiency, 2022, 29(3): 11-19.］

[14] Ma J, Wu C D, Wang Y Z, et al. Paleoenvironmental reconstruction of a saline lake in the Tertiary: Evidence from aragonite laminae in the northern Tibet Plateau[J]. Sedimentary Geology, 2017, 353: 1-12.

[15] Zhuang G S, Hourigan J K, Ritts B D, et al. Cenozoic multiple-phase tectonic evolution of the northern Tibetan Plateau: Constraints from sedimentary records from Qaidam Basin, Hexi Corridor, and Subei Basin, northwest China[J]. American Journal of Science, 2011, 311(2): 116-152.

[16] Stockhecke M, Anselmetti F S, Meydan A F, et al. The annual particle cycle in Lake Van (Turkey) [J]. Palaeogeography, Palaeoclimatology, Palaeoecology, 2012, 333-334: 148-159.

[17] Murphy Jr J T, Lowenstein T K, Pietras J T. Preservation of primary lake signatures in alkaline earth carbonates of the Eocene Green River Wilkins Peak-Laney member transition zone[J]. Sedimentary Geology, 2014, 314: 75-91.

[18] 毛玲玲,伊海生,季长军,等. 柴达木盆地新生代湖相碳酸盐岩岩石学及碳氧同位素特征[J]. 地质科技情报,2014,33（1）:41-48.［Mao Lingling, Yi Haisheng, Ji Changjun, et al. Petrography and carbon-oxygen isotope characteristics of the Cenozoic lacustrine carbonate rocks in Qaidam Basin[J]. Geological Science and Technology Information, 2014, 33(1): 41-48.］

[19] Andersson S, Rosqvist G, Leng M J, et al. Late Holocene climate change in central Sweden inferred from lacustrine stable isotope data[J]. Journal of Quaternary Science, 2010, 25(8): 1305-1316.

[20] Leng M J, Marshall J D. Palaeoclimate interpretation of stable isotope data from lake sediment archives[J]. Quaternary Science Reviews, 2004, 23(7/8): 811-831.

[21] Roeser P, Franz S O, Litt T. Aragonite and calcite preservation in sediments from Lake Iznik related to bottom lake oxygen-

ation and water column depth[J]. Sedimentology, 2016, 63(7): 2253-2277.

［22］ 黄成刚，倪祥龙，马新民，等. 致密湖相碳酸盐岩油气富集模式及稳产、高产主控因素：以柴达木盆地英西地区为例[J]. 西北大学学报（自然科学版），2017，47（5）：724-738.［Huang Chenggang, Ni Xianglong, Ma Xinmin, et al. Petroleum and gas enrichment pattern and major controlling factors of stable and high production of tight lacustrine carbonate rock reservoirs: A case of the Yingxi area in Qaidam Basin[J]. Journal of Northwest University (Natural Science Edition), 2017, 47(5): 724-738.］

［23］ 李翔，王建功，李飞，等. 柴达木盆地西部始新统湖相微生物岩沉积特征：以西岔沟和梁东地区下干柴沟组为例[J]. 岩性油气藏，2021，33（3）：63-73.［Li Xiang, Wang Jiangong, Li Fei, et al. Sedimentary characteristics of Eocene lacustrine microbialites in western Qaidam Basin: A case study from Xiaganchaigou Formation in Xichagou and Liangdong areas[J]. Lithologic Reservoirs, 2021, 33(3): 63-73.］

［24］ 王艳清，宋光永，刘占国，等. 柴达木盆地新生代咸化湖盆碳酸盐岩类型及发育特征[J]. 中国石油大学学报（自然科学版），2020，44（1）：1-13.［Wang Yanqing, Song Guangyong, Liu Zhanguo, et al. Carbonate types and developmental patterns of Cenozoic saltwater lake basin in Qaidam Basin[J]. Journal of China University of Petroleum, 2020, 44(1): 1-13.］

［25］ 朱超，刘占国，宋光永，等. 柴达木盆地英雄岭构造带古近系湖相碳酸盐岩沉积模式、演化与分布[J]. 石油学报，2022，43（11）：1558-1567，1622.［Zhu Chao, Liu Zhanguo, Song Guangyong, et al. Sedimentary model, evolution and distribution of Paleogene lacustrine carbonate rocks in Yingxiongling structural belt, Qaidam Basin[J]. Acta Petrolei Sinica, 2022, 43(11): 1558-1567, 1622.］

［26］ 宋光永，朱超，李森明，等. 柴达木盆地英西地区湖相混积型碳酸盐岩储层成因及发育模式[J]. 中国石油大学学报（自然科学版），2022，46（3）：1-12.［Song Guangyong, Zhu Chao, Li Senming, et al. Genetic mechanism and development model of lacustrine hybrid carbonate reservoirs in the western Yingxiongling structural belt, Qaidam Basin[J]. Journal of China University of Petroleum (Edition of Natural Science), 2022, 46(3): 1-12.］

［27］ 李树峰，星耀武，Valdes P J，等. 欧亚大陆渐新世古气候时空演变及其驱动因子：基于植物大化石和气候模型的综合分析[C]//中国古生物学会第十二次全国会员代表大会暨第29届学术年会论文摘要集. 郑州：中国古生物学会，2018.［Li Shufeng, Xing Yaowu, Valdes P. J., et al. Comprehensive analysis of the spatial and temporal evolution of paleoclimate in the Eurasian continent during the Eocene and its driving factors: Based on plant macrofossils and climate models [C]// Abstracts of the 12th National Member Representative Conference of the Chinese Paleontological Society and the 29th Annual Academic Meeting. Zhengzhou: Chinese Paleontological Society,

2018.］

［28］ 宋华颖，伊海生，范爱春，等. 柴达木盆地西部西岔沟剖面湖相碳酸盐岩岩石学特征与沉积环境分析[J]. 中国地质，2010，37（1）：117-126.［Song Huaying, Yi Haisheng, Fan Aichun, et al. Petrology and sedimentary environments of lacustrine carbonate rocks in the Xichagou section, western Qaidam Basin[J]. Geology in China, 2010, 37(1): 117-126.］

［29］ Guo P, Liu C Y, Huang L, et al. Palaeohydrological evolution of the Late Cenozoic saline lake in the Qaidam Basin, NE Tibetan Plateau: Tectonic vs. climatic control[J]. Global and Planetary Change, 2018, 165: 44-61.

［30］ 崔俊，毛建英，陈登钱，等. 柴达木盆地西部地区古近系湖相碳酸盐岩储层特征[J]. 岩性油气藏，2022，34（2）：45-53.［Cui Jun, Mao Jianying, Chen Dengqian, et al. Reservoir characteristics of Paleogene lacustrine carbonate rocks in western Qaidam Basin[J]. Lithologic Reservoirs, 2022, 34(2): 45-53.］

［31］ 秦胜飞，秦勇，钟宁宁，等. 碳酸盐岩中有机质赋存分类[J]. 石油勘探与开发，1996，23（6）：23-27.［Qin Shengfei, Qin Yong, Zhong Ningning, et al. Classification on occurrence of organic matter in carbonate rocks[J]. Petroleum Exploration and Development, 1996, 23(6): 23-27.］

［32］ 袁剑英，黄成刚，曹正林，等. 咸化湖盆白云岩碳氧同位素特征及古环境意义：以柴西地区始新统下干柴沟组为例[J]. 地球化学，2015，44（3）：254-266.［Yuan Jianying, Huang Chenggang, Cao Zhenglin, et al. Carbon and oxygen isotopic composition of saline lacustrine dolomite and its palaeoenvironmental significance: A case study of Lower Eocene Ganchaigou Formation in western Qaidam Basin[J]. Geochimica, 2015, 44(3): 254-266.］

［33］ Talbot M R, Kelts K. Paleolimnological signatures from carbon and oxygen isotopic ratios in carbonates from organic carbon-rich lacustrine sediments[M]//Katz B J. Lacustrine basin exploration: Case studies and modern analogs. Tulsa: American Association of Petroleum Geologists, 1990.

［34］ 于冬冬，张永生，邢恩袁，等. 柴达木西部南翼山构造地表混积岩岩石学特征及沉积环境讨论[J]. 地质学报，2018，92（10）：2068-2080.［Yu Dongdong, Zhang Yongsheng, Xing Enyuan, et al. Petrological characteristics and sedimentary environment of the surface mixed rocks in Nanyishan structure, western Qaidam Basin[J]. Acta Geologica Sinica, 2018, 92(10): 2068-2080.］

［35］ 年秀清. 柴达木盆地西部富锶地层的地球化学特征及其地质意义[D]. 西宁：中国科学院大学（中国科学院青海盐湖研究所），2018.［Nian Xiuqing. Geochemical characteristics of the rich strontium stratum in western Qaidam Basin and it's geological significance[D]. Xining: University of Chinese Academy of Sciences (Qinghai Institute of Salt Lakes, Chinese Academy of Sciences), 2018.］

［36］ Jian X, Guan P, Fu S T, et al. Miocene sedimentary environment and climate change in the northwestern Qaidam Basin,

northeastern Tibetan Plateau: Facies, biomarker and stable isotopic evidences[J]. Palaeogeography, Palaeoclimatology, Palaeoecology, 2014, 414: 320-331.

［37］ 赵加凡，陈小宏，金龙. 柴达木盆地第三纪盐湖沉积环境分析[J]. 西北大学学报（自然科学版），2005，35（3）：342-346.［Zhao Jiafan, Chen Xiaohong, Jin Long. Application of stable isotope in Tertiary saline lake of Qaidamu Basin[J]. Journal of Northwest University (Natural Science Edition), 2005, 35(3): 342-346.］

［38］ 纪友亮，马达德，薛建勤，等. 柴达木盆地西部新生界陆相湖盆碳酸盐岩沉积环境与沉积模式[J]. 古地理学报，2017，19（5）：757-772.［Ji Youliang, Ma Dade, Xue Jianqin, et al. Sedimentary environments and sedimentary model of carbonate rocks in the Cenozoic lacustrine basin, western Qaidam Basin [J]. Journal of Palaeogeography, 2017, 19(5): 757-772.］

［39］ 肖路安. 柴达木盆地新生代碳酸盐岩碳氧同位素特征及其古气候意义[D]. 兰州：兰州大学，2022.［Xiao Lu'an. Carbon and oxygen isotope characteristics of Cenozoic carbonate rocks in Qaidam Basin and their paleoclimate significance[D]. Lanzhou: Lanzhou University, 2022.］

［40］ 刘占国，张永庶，宋光永，等. 柴达木盆地英西地区咸化湖盆混积碳酸盐岩岩相特征与控储机制[J]. 石油勘探与开发，2021，48（1）：68-80.［Liu Zhanguo, Zhang Yongshu, Song Guangyong, et al. Mixed carbonate rocks lithofacies features and reservoirs controlling mechanisms in the saline lacustrine basin in Yingxi area, Qaidam Basin, NW China[J]. Petroleum Exploration and Development, 2021, 48(1): 68-80.］

［41］ Zhou A F, Chen F H, Qiang M R, et al. The discovery of annually laminated sediments (varves) from shallow Sugan Lake in inland arid China and their paleoclimatic significance[J]. Science China Earth Sciences, 2007, 50(8): 1218-1224.

［42］ Wen Y X, Sánchez-Román M, Li Y L, et al. Nucleation and stabilization of Eocene dolomite in evaporative lacustrine deposits from central Tibetan Plateau[J]. Sedimentology, 2020, 67 (6): 3333-3354.

［43］ Bruce W. Boyer. Tertiary lacustrine sediments from sentinel butte, North Dakota and the sedimentary record of ectogenic meromixis[J]. Journal of Sedimentary Research, 1981, 51(2): 429-440.

［44］ Jackson M J. Mid-Proterozoic dolomitic varves and microcycles from the McArthur Basin, northern Australia[J]. Sedimentary Geology, 1985, 44(3/4): 301-326.

［45］ Prasad S, Negendank J F W, Stein M. Varve counting reveals high resolution radiocarbon reservoir age variations in Palaeolake Lisan[J]. Journal of Quaternary Science, 2009, 24(7): 690-696.

［46］ Kelts K, Hsü K J. Freshwater carbonate sedimentation[M]//Lerman A. Lakes: Chemistry, geology, physics. New York: Springer, 1978: 295-323.

［47］ Burton E A, Walter L M. Relative precipitation rates of aragonite and Mg calcite from seawater: Temperature or carbonate ion control?[J]. Geology, 1987, 15(2): 111-114.

［48］ Berner R A. The role of magnesium in the crystal growth of calcite and aragonite from sea water[J]. Geochimica et Cosmochimica Acta, 1975, 39(4): 489-504.

［49］ 陈能贵，王艳清，徐峰，等. 柴达木盆地新生界湖盆咸化特征及沉积响应[J]. 古地理学报，2015，17（3）：371-380.［Chen Nenggui, Wang Yanqing, Xu Feng, et al. Palaeosalinity characteristics and its sedimentary response to the Cenozoic saltwater lacustrine deposition in Qaidam Basin[J]. Journal of Palaeogeography, 2015, 17(3): 371-380.］

［50］ Guo P, Liu C Y, Yu M L, et al. Paleosalinity evolution of the Paleogene perennial Qaidam Lake on the Tibetan Plateau: Climatic vs. tectonic control[J]. International Journal of Earth Sciences, 2018, 107(5): 1641-1656.

［51］ Swart P K. The geochemistry of carbonate diagenesis: The past, present and future[J]. Sedimentology, 2015, 62(5): 1233-1304.

［52］ Folk R L, Land L S. Mg/Ca ratio and salinity: Two controls over crystallization of dolomite[J]. AAPG Bulletin, 1975, 59 (1): 60-68.

［53］ Huguet C, Fietz S, Stockhecke M, et al. Biomarker seasonality study in lake van, Turkey[J]. Organic Geochemistry, 2011, 42 (11): 1289-1298.

［54］ Song B W, Spicer R A, Zhang K X, et al. Qaidam Basin leaf fossils show northeastern Tibet was high, wet and cool in the Early Oligocene[J]. Earth and Planetary Science Letters, 2020, 537: 116175.

［55］ Casella L A, Griesshaber E, Yin X F, et al. Experimental diagenesis: Insights into aragonite to calcite transformation of *Arctica islandica* shells by hydrothermal treatment[J]. Biogeosciences, 2017, 14(6): 1461-1492.

［56］ Casella L A, He S X, Griesshaber E, et al. Hydrothermal alteration of aragonitic biocarbonates: Assessment of micro- and nanostructural dissolution – reprecipitation and constraints of diagenetic overprint from quantitative statistical grain-area analysis[J]. Biogeosciences, 2018, 15(24): 7451-7484.

［57］ Gerhardt S, Groth H, Rühlemann C, et al. Aragonite preservation in Late Quaternary sediment cores on the Brazilian continental slope: Implications for intermediate water circulation[J]. International Journal of Earth Sciences, 2000, 88(4): 607-618.

［58］ Nohl T, Wetterich J, Fobbe N, et al. Lithological dependence of aragonite preservation in monospecific gastropod deposits of the Miocene Mainz Basin: Implications for the (dia-)genesis of limestone-marl alternations[J]. Journal of Sedimentary Research, 2020, 90(11): 1500-1509.

［59］ 李维，朱筱敏，段宏亮，等. 苏北盆地高邮—金湖凹陷古近系阜宁组细粒沉积岩纹层特征与成因[J]. 古地理学报，2020，22（3）：469-482.［Li Wei, Zhu Xiaomin, Duan Hongliang, et al. Characteristics and forming mechanism of laminae

fine-grained sedimentary rock of the Paleogene Funing Formation in Gaoyou and Jinhu sags, Subei Basin[J]. Journal of Palaeogeography, 2020, 22(3): 469-482.］

［60］ Keith M L, Weber J N. Carbon and oxygen isotopic composition of selected limestones and fossils[J]. Geochimica et Cosmochimica Acta, 1964, 28(10/11): 1787-1816.

［61］ 任雪瑶,谭先锋,张晨晨,等. 湖相碳酸盐岩白云石化流体来源、作用机制及物质过程[J]. 地质找矿论丛,2018,33（1）:76-85.［Ren Xueyao, Tan Xianfeng, Zhang Chenchen, et al. Source of dolomitization fluid, mechanism and material process of lacustrine carbonate rocks[J]. Contributions to Geology and Mineral Resources Research, 2018, 33(1): 76-85.］

［62］ 王兵杰,蔡明俊,林春明,等. 渤海湾盆地塘沽地区古近系沙河街组湖相白云岩特征及成因[J]. 古地理学报,2014,16（1）:65-76.［Wang Bingjie, Cai Mingjun, Lin Chunming, et al. Characteristics and origin of lacustrine dolostone of the Paleogene Shahejie Formation in Tanggu area, Bohai Bay Basin[J]. Journal of Palaeogeography, 2014, 16(1): 65-76.］

［63］ Song Y G, Zong X L, Qian L B, et al. Mineralogical record for stepwise hydroclimatic changes in lake Qinghai sediments since the last glacial period[J]. Minerals, 2020, 10(11): 963.

［64］ 李进龙,陈东敬. 古盐度定量研究方法综述[J]. 油气地质与采收率,2003,10（5）:1-3.［Li Jinlong, Chen Dongjing. Summary of quantified research method on paleosalinity[J]. Petroleum Geology and Recovery Efficiency, 2003, 10(5): 1-3.］

［65］ Huang X T, Oberhänsli H, von Suchodoletz H, et al. Hydrological changes in western central Asia (Kyrgyzstan) during the Holocene as inferred from a palaeolimnological study in Lake Son Kul[J]. Quaternary Science Reviews, 2014, 103: 134-152.

［66］ Smith M E, Carroll A R, Scott J J, et al. Early Eocene carbon isotope excursions and landscape destabilization at eccentricity minima: Green River Formation of Wyoming[J]. Earth and Planetary Science Letters, 2014, 403: 393-406.

［67］ McCormack J, Nehrke G, Jöns N, et al. Refining the interpretation of lacustrine carbonate isotope records: Implications of a mineralogy-specific Lake Van case study[J]. Chemical Geology, 2019, 513: 167-183.

［68］ Wu M H, Zhuang G S, Hou M Q, et al. Expanded lacustrine sedimentation in the Qaidam Basin on the northern Tibetan Plateau: Manifestation of climatic wetting during the Oligocene icehouse[J]. Earth and Planetary Science Letters, 2021, 565: 116935.

Formation of Carbonate Laminae in the Oligocene Shangganchaigou Formation of the Qaidam Basin and Its Paleoclimatic Significance

HE HaiLong[1,2,3], GUO Pei[1,2,3], LI ChangZhi[2,4], WEI Yan[3], ZHANG XiTing[1,2,3], WEN HuaGuo[1,2,3]

1. Key Laboratory of Deep-time Geography and Environment Reconstruction and Applications of Ministry of Natural Resources, Chengdu University of Technology, Chengdu 610059, China

2. State Key Laboratory of Oil and Gas Reservoir Geology and Exploitation, Chengdu University of Technology, Chengdu 610059, China

3. Institute of Sedimentary Geology, Chengdu University of Technology, Chengdu 610059, China

4. School of Earth Sciences, Chengdu University of Technology, Chengdu 610059, China

Abstract：［**Objective**］Laminations are sedimentary structures that result from the slow deposition of fine-grained materials under stratified conditions in lakes. Among the various types of laminations, carbonate laminations are particularly sensitive indicators of changes in water salinity, alkalinity, and biological activity. They supply important evidence for reconstructing past continental climates and hydrology, and the study of lacustrine carbonate laminations can provide valuable information on the evolution of lake systems and associated environmental changes. However, research on lacustrine carbonate laminations has been relatively limited. By studying the lacustrine carbonate laminations in the Qaidam Basin, particularly the genesis of aragonite and calcite in the carbonate laminations and the mechanisms of their formation, we aim to reveal the climate and environmental changes in the northern Tibetan Plateau during the Eocene.［**Methods**］Taking the Upper Oligocene Gangchaigou Formation in the Xichagou section of the Qaidam Basin as an example, we conducted observations using conventional thin sections, fluorescence thin sections, and scanning electron microscopy, as well as X-ray powder diffraction and carbon-oxygen isotope analysis. Based on the analysis of petrological and carbon-oxygen isotopic characteristics, we investigated the vertical

variations of carbonate mineral content and carbon-oxygen isotopes in the Gangchaigou Formation of the Xichagou section.［**Results**］The Gangchaigou Formation in the Xichagou section consists of three types of laminations：silt, carbonate, and clay. Among them, aragonite, calcite, and dolomite are alternately enriched in the carbonate laminations. Samples with high aragonite content have relatively positive carbon isotope ratios, whereas samples enriched in dolomite have relatively higher oxygen isotope ratios. Moreover, there are certain regularities in the vertical variations of carbonate mineral content and carbon-oxygen isotopes in the Gangchaigou Formation in the Xichagou section. ［**Conclusion**］（1）The Upper Gangchaigou Formation in the Qaidam Basin contains various types of lacustrine laminations, primarily interbedded carbonate and feldspar laminations. The mineral compositions of most laminations are impure, with a mixture of terrestrial debris and authigenic carbonate minerals.（2）The formation and preservation of aragonite, calcite, and dolomite in the laminations of the Upper Gangchaigou Formation are related to the chemical composition of the water（such as the Mg/Ca ratio）and algal biological activity. Under the overall brackish water environment, when the external water supply exceeds the evaporation rate, the Mg/Ca value in the water decreases, the salinity decreases, and the nutrient input increases. As a result, calcite and aragonite minerals begin to precipitate and transform. The preservation of aragonite in the Eocene strata is related to the blooming of algae and the abundance of organic matter. When the evaporation rate exceeds the water supply, the Mg/Ca value in the water increases, the salinity increases, and dolomite forms through the replacement of calcite or aragonite or by precipitation.（3）During the Eocene, the climate in the Qaidam Basin was consistent with global climate change, with a humid climate prevailing in the early period and a semi-arid climate prevailing in the late period. The lakes in the Xichagou area experienced an evolution from low to high water levels and then back to low water levels. The early low water level stage represents shallow, brackish water sedimentation with a high input of terrestrial debris. The middle high water level stage represents brackish water sedimentation with well-developed calcite and aragonite. The late low water level stage represents shallow, saline water sedimentation with a low input of terrestrial debris.

Key words：lacustrine lamination；aragonite；dolomite；algal bloom；paleohydrology